

Improved Hessian Method in Global Analysis of Parton Distribution Functions

WenXiao Zhan, Siqi Yang,^{*} Minghui Liu, and Liang Han

Department of Modern Physics, University of Science and Technology of China, Jinzhai Road 96, Hefei, Anhui 230026, China

Daniel Stump and C.-P. Yuan

Department of Physics and Astronomy, Michigan State University, East Lansing, MI 48823, USA

The Hessian method is widely applied in the global analysis of parton distribution functions (PDFs), which uses a set of orthogonal eigenvectors to give predictions of a physical observable. Its uncertainty is estimated based on the assumption that all physical observables can be approximately expressed as linear functions of the non-perturbative parameters in PDF. In this article, we report an improved Hessian method which takes the non-linear effects into account in the uncertainty estimation. A pseudo global analysis is designed to numerically test the new method. The non-linear uncertainties can significantly enlarge the original linear ones. Such uncertainties can be reduced with high precision data introduced into the global analysis. However, the non-linear effect could still be sizable corresponding to the current precision of the experimental measurements.

I. INTRODUCTION

In the past decades, a global analysis method based on quantum chromodynamics (QCD) has been established to study the proton structure at high energy scale. It sufficiently analyzes comprehensive data results from the deep inelastic scattering (DIS) experiments with the energy scale of a few GeV, to the processes at hadron colliders at $\mathcal{O}(100)$ GeV. The global analysis is expected to not only give the central predictions on parton densities corresponding to the best fit of the data, but also provide a way that the uncertainties can be easily calculated and extrapolated for any particular physical observable. The Hessian method [1] is one of the most widely used strategies to estimate the PDF uncertainties, such as in the latest CT18NNLO and MSHT20 PDFs [2, 3]. In this approach, a group of error PDF sets are provided, which represent the possible variations on the parameters of the non-perturbative functions of the quarks and gluons. These error sets correspond to orthogonal eigenvectors in the original parameter space, so that the uncertainty of a particular physical observable can be calculated using the error sets without complicated analysis on the correlations between the original parameters.

In the current Hessian method, the uncertainty estimation is established as a linear approximation. Firstly, the orthogonal eigenvectors and their corresponding uncertainties are determined by assuming the physical observables of those data used in the global analysis can be expressed as linear functions of the non-perturbative PDF parameters. Secondly, when computing the PDF-induced uncertainty on a given physical observable using the eigenvectors, the observable is also assumed as linear function of the eigenvectors. The non-linear effects, appearing as the higher order derivatives in the expansion of physical observables as functions of PDF parameters or eigenvectors, are ignored. Such effect could be significant

in high energy interactions, such as the LHC which provides precise experimental results in today's PDF global analysis. A few previous studies have been performed on the non-linearities in the global analysis. For example, Ref. [4] discussed contributions from the second-order terms based on the CT14 PDFs [5], but only for those appearing as the diagonal elements in the Hessian matrix (as to be introduced later). Based on the same PDFs, it was found later in Ref. [6] that the diagonal higher order terms could be sizable in the analysis of the CMS di-jet measurement.

In this work, we introduce an improved Hessian method, in which the non-linear effects are estimated as additional uncertainties. To make a detailed comparison between the improved method and the original one, a pseudo global fit is studied. As will be demonstrated in this test, the uncertainty on parton densities could be noticeably different from the original linear estimation. Such difference can be reduced as the precision of the input data in the global analysis improves. However, the needed precision to reduce the non-linear uncertainties to negligible level is far beyond the current precision of experimental observations.

The article will be arranged as following: In section II, we review the general strategy of Hessian method; In section III, we discuss the non-linear effects in the global analysis; In section IV, we introduce the improved method to estimate the non-linear uncertainties; In section V, we perform a pseudo global analysis study to numerically test the improved method, and summarize the conclusion of this article.

II. THE ORIGINAL HESSIAN METHOD

In this section, we review the original Hessian method [1] and its linear uncertainty estimation. In Hes-

sian method, a series of non-perturbative functions are introduced to describe the parton densities at the scale of Q_0 . Taking from the CT18NNLO PDF as an example, the functions are written in the formalism as:

$$f_q(x, Q_0) = a_0 x^{a_1-1} (1-x)^{a_2} P_q(x; a_3, a_4, \dots) \quad (1)$$

where x is the momentum fraction of the parton q inside the proton. P_q is a polynomial designed to allow the parton density to change its shape in order to match the data inputs in different x regions. $\{a_i\}$ are the original parameters being determined in the global fit, by minimizing the χ^2 defined as:

$$\chi^2 = \sum_{\alpha} \frac{[D_{\alpha} - T_{\alpha}(\{a_i\})]^2}{\sigma_{\alpha}^2} \quad (2)$$

where D_{α} and σ_{α} are the experimental inputs and their corresponding uncertainties. $T_{\alpha}(a_i)$ is the theory prediction of D_{α} , depending on the PDF shape parameters $\{a_i\}$. Given the fact that the best fit values of $\{a_i\}$ appear near the minimal χ^2 , we have:

$$\chi^2 = \chi_{\min}^2 + \frac{1}{2} \sum_{i,j} \frac{\partial^2 \chi^2}{\partial a_i \partial a_j} (a_i - a_i^0)(a_j - a_j^0) + \dots \quad (3)$$

The Hessian matrix is then defined as $H_{ij} = \partial^2 \chi^2 / \partial a_i \partial a_j$. Note that $\{a_i\}$ are quite independent as free parameters in the non-perturbative functions, but their uncertainties in a global analysis can be correlated because experimental observables usually relate to multiple PDF shape parameters. The correlation depends on the particular set of experimental inputs used in a global fit. One can convert $\{a_i\}$ to another set of orthogonal parameters $\{z_i\}$ by diagonalizing H_{ij} :

$$\sum_j H_{ij} v_{jk} = \epsilon_k v_{ik},$$

where ϵ_k are the eigenvalues and v_{ik} are the orthogonal and complete eigenvectors. Then, the displacements of $\{a_i\}$ are given as

$$a_i - a_i^0 = \sum_k v_{ik} s_k z_k, \quad (4)$$

where the scaling factors $\{s_i\}$ are introduced to normalize $\{z_i\}$. Usually, $\{s_i\}$ are chosen to make

$$\Delta \chi^2 = \chi^2 - \chi_{\min}^2 = \sum_i z_i^2, \quad (5)$$

so that the best fit of χ^2 (denoted as χ_{\min}^2) corresponds to $\{z_i = 0\}$, and the one-standard deviation uncertainty in the direction of the i -th eigenvector corresponds to $\{z_i = \pm 1; z_j = 0 \text{ for } j \neq i\}$. By this requirement, $\{s_i\}$ are approximately equal to $\sqrt{2/\epsilon_i}$.

In practice, χ^2 is more complicated, which may include correlated systematical uncertainties. Furthermore, the one-standard deviation uncertainty is usually enlarged by some dynamical and/or global tolerances to deal with the possible inconsistency between data, and to cover the uncertainty due to the choice of the non-perturbative parameterizations. For simplicity, we ignore all these variants in this work as they will not strongly alter our conclusions.

For a given physical observable whose theory prediction depends on PDFs, it can be expanded as:

$$\mathcal{O}(\{z_i\}) = \mathcal{O}(\{z_i^0\}) + \sum_i \left. \frac{\partial \mathcal{O}}{\partial z_i} \right|_{z_i^0} dz_i + \frac{1}{2} \sum_{i,j} \left. \frac{\partial^2 \mathcal{O}}{\partial z_i \partial z_j} \right|_{z_i^0, z_j^0} dz_i dz_j + \dots \quad (6)$$

As $\{z_i\}$ represent orthogonal eigenvectors, the leading order uncertainty on \mathcal{O} can simply be calculated as:

$$\delta \mathcal{O} \approx \sqrt{\sum_i \left[\frac{\mathcal{O}(z_i^0 + \delta z_i) - \mathcal{O}(z_i^0 - \delta z_i)}{2\delta z_i} \right]^2} \quad (7)$$

where $\delta z_i = 1$ is the uncertainty on z_i . $\mathcal{O}(z_i^0 \pm \delta z_i)$ is the calculation of \mathcal{O} where the value of the i -th parameter is shifted by $\pm \delta z_i$, while all other parameters $z_j (j \neq i)$ are fixed at their central values z_j^0 . To enable the calculation, the global analysis provides a central PDF set $S_0 = S(\{z_i^0\})$ which can be used to calculate the central prediction of $\mathcal{O}(S_0)$, and a group of error PDF sets $S_{i\pm} = S(z_i^0 \pm \delta z_i; z_j = z_j^0 \text{ for } j \neq i)$. Hence, the uncertainty in Eq. (7) can be calculated using the PDF error sets:

$$\delta \mathcal{O} = \sqrt{\sum_i \left(\frac{\mathcal{O}(S_{i+}) - \mathcal{O}(S_{i-})}{2} \right)^2} \quad (8)$$

III. NON-LINEAR EFFECTS IN GLOBAL ANALYSIS

The first linear assumption in the original Hessian method is introduced in the determination of the eigenvectors and their uncertainties. The orthogonal parameters $\{z_i\}$ are acquired using the Hessian matrix containing only the $\partial^2 \chi^2 / \partial a_i \partial a_j$ terms. The one standard deviation is defined as $\delta z_i = 1$ corresponding to $\Delta \chi^2 = 1$. All these settings are based on the assumption that the physical observables of the data used in the global analysis can be written as the linear functions of the original PDF parameters $\{a_i\}$:

$$T_{\alpha}(\{a_i\}) = \sum_i t_{\alpha}^i a_i \quad (9)$$

where t_{α}^i is the coefficient. In principle, Eq. (9) never holds true in global analysis. Firstly, the non-perturbative functions in Eq. (1) are naturally non-linear, e.g. the power terms x^{1-a_1} and $(1-x)^{a_2}$ which are guided by the Regge theory [7] and the spectator counting rules [8] to describe the asymptotic behavior of $f_q(x)$ in the limits $x \rightarrow 0$ and 1. Secondly, the calculations on physical interactions are usually convolutions over x . Thirdly, for those collider and fixed target experiments, the calculations on the two-hadron initial state contain the product of the two parton densities. In practice, when data inputs used in a global analysis have high precisions, $\Delta \chi^2$ would increase rapidly as $\{a_i\}$ values running away from their best fitted values. Thus, all calculations can be

done in small intervals around $\{a_i^0\}$ so that $T_\alpha(\{a_i\})$ can be numerically linear. In other words, the non-linearity depends on the precision of the experimental measurements in the PDF global analysis. In current PDFs, the experimental inputs provide good constraints in some x regions and for the quark flavors that they are sensitive to. However, the data precisions in the foreseeable future would not be good enough to suppress the non-linear effect for all quark flavors and in a wide range of x .

Another linear assumption is introduced in computing the PDF-induced uncertainties on physical observables using the eigenvectors. In the current Hessian method, the higher order contributions in Eq. (6) are ignored when extrapolating the uncertainties on eigenvectors to a given physical observable. The Hessian-type PDFs such as CT18 and MSHT20 provide only the error sets $S_{i\pm}$ corresponding to the complete differential of z_i , which allows calculation of $\partial\mathcal{O}/\partial z_i$, $\partial^2\mathcal{O}/\partial z_i^2$ or even higher order contributions as the diagonal elements. But these error sets cannot give estimations on the non-linear terms such as $\partial^2\mathcal{O}/\partial z_i\partial z_j$. The higher order contributions can be significant especially when the computed physical observable corresponds to x region or quark flavor very differently from that of the data in the global fit.

In CT18 [2], the uncertainties of the PDF error sets are quoted to cover the difference from varying the formalism of the non-perturbative functions of Eq. (1). By doing this, CT18 gives more conservative uncertainty estimation compared to MSHT20 [3] and NNPDF4 [10], which use similar data set in the global fit. The enlarged uncertainties reflect the non-linear effects in global analysis, because if the non-perturbative functions tested by CT18 were all in good linear approximation, they would lead to consistent predictions on any physical observable because they were connected by linear transformations in the PDF parameter space. In other words, it is, to some extent, similar to estimating the uncertainty due to the non-linearity with respect to the uncertainty due to the particular choice of non-perturbative functions used in the global fit. However, it is inevitable in the enumeration method that many functions being tested are known to have disadvantages in describing the data. Consequently, the uncertainty may be overestimated by quoting the imperfection of the excluded functions rather than the imperfection of the chosen function. On the other hand, the uncertainty may also be underestimated as there is always possible functions missed in the enumeration. Therefore, a new method to estimate the uncertainty of the chosen function itself would be important.

IV. IMPROVED HESSIAN METHOD

The improved method will be derived in this Section. Then, in Section V we will apply it to a pseudo analysis,

to test how non-linear contributions can affect a global analysis. The pseudo-linear calculation will be compared to the nominal (un-improved) global fit.

The strategy is as following:

i) For a given non-perturbative function formalism such as in Eq. (1), perform the global analysis with the normal method, giving the best fitted values of $\{a_i = a_i^0\}$ and the central PDF set S_0 . In this nominal fit, $T_\alpha(\{a_i\})$ are predicted with different $\{a_i\}$ inputs based on the conventional calculations.

ii) For each physical observable, a set of linear factors are defined as:

$$K_i^\alpha = \frac{T_\alpha^{i+} - T_\alpha^{i-}}{2\epsilon_i}. \quad (10)$$

where $T_\alpha^{i+} = T_\alpha(\{a_i = a_i^0 + \epsilon_i; a_j = a_j^0 \text{ for } i \neq j\})$ and $T_\alpha^{i-} = T_\alpha(\{a_i = a_i^0 - \epsilon_i; a_j = a_j^0 \text{ for } i \neq j\})$. Apparently, K_i^α is an approximation of $\partial T_\alpha(\{a_i\})/\partial a_i$ around $\{a_i = a_i^0\}$ in the range of $(a_i - \epsilon_i, a_i + \epsilon_i)$. It represents the slope of the secant line, as shown in Fig. 1. The ϵ_i parameter corresponds to the range of a_i in which the linear derivation of Eq. (10) is assumed. Thus, ϵ_i can simply be set to the original uncertainty of the a_i parameter given by the fit obtained from i).

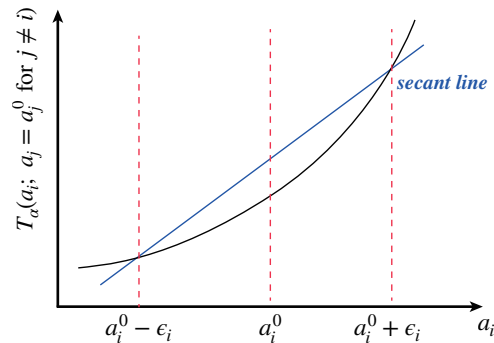


FIG. 1. The secant line of $T_\alpha(a_i; a_j = a_j^0 \text{ for } j \neq i)$ around the best fitted value a_i^0 .

iii) A group of new observables can then be established as linear functions of $\{a_i\}$:

$$T_\alpha^{(r)}(\{a_i\}) = T_\alpha(\{a_i^r\}) + \sum_i K_i^\alpha \times (a_i - a_i^r), \quad (11)$$

where $\{a_i^r\}$, $r = 0, 1, \dots, n$ represent a set of points in the parameter space of $\{a_i\}$, with n as the number of the parameters. Values of $\{a_i^r\}$ also represent the range of the linear assumption, but in terms of T_α . In order to achieve this, $\{a_i^r\}$ values can be set corresponding to $\{z_r = \Delta_r; z_i = 0 \text{ for } i \neq r\}$. Δ_r is chosen to have $T_\alpha(\{a_i^r\}) - T_\alpha(\{a_i^0\})$ consistent with σ_α for those data inputs sensitive to z_r . Note that when the eigenvector z_r is constrained by multiple data inputs in the global fit, the uncertainty of z_r (δz_r) will be smaller than Δ_r , since δz_r reflects the combination of the statistical power of those data inputs.

Using Eq. (11), one can perform a linear fit, in which the best values of $\{a_i\}$ are determined by requiring the minimum of $\chi^2(T^{(r)})$ defined as:

$$\chi^2(T^{(r)}) = \sum_{\alpha} \frac{[D_{\alpha} - T_{\alpha}^{(r)}(\{a_i\})]^2}{\sigma_{\alpha}^2}. \quad (12)$$

When Eq. (9) is in good approximation, the linear fit using Eq. (12) would give best fit values, denoted as $\{a_i^{r,0}\}$ for each r , consistent with the nominal fit $\{a_i^0\}$. Therefore, the difference between the two fits reflects the non-linearity of the physical observables $T_{\alpha}(\{a_i\})$, and can be quoted as additional uncertainties. To do this, an additional PDF error set is defined as $S_E(r) = S(\{a_i^{r,0}\})$ for each eigenvector. For a given physical observable \mathcal{O} , the non-linear uncertainty is defined as:

$$\delta\mathcal{O}_E = \sqrt{\sum_r [\mathcal{O}(S_E(r)) - \mathcal{O}(S_0)]^2} \quad (13)$$

It should be emphasized that Eq. (13) quantifies the impact on non-linearity when extrapolated to a physical observable. Such non-linearity introduces a bias in the analysis, which may in turn contribute to the PDF uncertainty. The notions of “bias” and “uncertainty” are not strictly equivalent, although they are likely to be of comparable size. A more detailed analysis would be required to establish their precise relationship in a specific case. $\delta\mathcal{O}_E$ is the uncertainty of assuming $T_{\alpha}(\{a_i\})$ as linear functions, which is independent of how to extrapolate the original experimental uncertainties σ_{α} to each eigenvector, and further to a physical observable \mathcal{O} . As discussed in the section II, the error sets $S_{i\pm}$ allow calculations only on the first-order derivatives in Eq. (6). Below, we show how to obtain the PDF error sets for calculating the full second-order derivatives. Following the definition of the derivative, the needed error sets are:

$$S_{j\pm}^{i\pm} = S(z_i = \pm 1, z_j = \pm 1; z_k = 0 \text{ for } k \neq i, j), \quad (14)$$

in which two displacements are varied simultaneously, so that the second-order derivatives can be calculated as:

$$\frac{\partial^2 \mathcal{O}}{\partial z_i \partial z_j} = \frac{1}{2} \times \left(\frac{\mathcal{O}(S_{j+}^{i+}) - \mathcal{O}(S_{j+}^{i-})}{2} - \frac{\mathcal{O}(S_{j-}^{i+}) - \mathcal{O}(S_{j-}^{i-})}{2} \right) \quad (15)$$

For $i = j$, the second-order error sets can be calculated as $S_{i++} = S(z_i = 2; z_k = 0 \text{ for } k \neq i)$ and $S_{i--} = S(z_i = -2; z_k = 0 \text{ for } k \neq i)$. Consequently, we have

$$\frac{\partial^2 \mathcal{O}}{\partial z_i^2} = \frac{1}{2} \times \left(\frac{\mathcal{O}(S_{i++}) - \mathcal{O}(S_0)}{2} - \frac{\mathcal{O}(S_0) - \mathcal{O}(S_{i--})}{2} \right) \quad (16)$$

According to Eq. (4), the values of the original parameters $\{a_i\}$ corresponding to $\{z_i = \pm 1, z_j = \pm 1; z_k = 0 \text{ for } k \neq i, j\}$ can be calculated, and thus the second-order error sets $S_{j\pm}^{i\pm}$ can be directly generated. Since the Hessian matrix comes from the derivatives of χ^2 , the second-order error sets can only be acquired together with the

first-order error sets in a complete PDF global analysis. With the full second-order derivatives included, the uncertainty on \mathcal{O} is written as:

$$(\delta\mathcal{O})^2 = \sum_i \left(\frac{\partial \mathcal{O}}{\partial z_i} \right)^2 + \frac{1}{2} \sum_i \left(\frac{\partial^2 \mathcal{O}}{\partial z_i^2} \right)^2 + \frac{1}{2} \sum_{i \neq j} \left(\frac{\partial^2 \mathcal{O}}{\partial z_i \partial z_j} \right)^2, \quad (17)$$

where the first, second and third terms correspond to the contributions from the first-order derivatives, the second-order diagonal derivatives, and the second-order off-diagonal derivatives in Eq. (6), respectively. The process of proof of Eq. (17) is given in the Appendix.

One can also calculate the uncertainty in an alternative way:

i) give each displacement z_i (along each eigenvector v_i) a random value according to the normalized gaussian distribution $G(0, 1)$.

ii) calculate $\mathcal{O} = \mathcal{O}(S_0) + \sum_i \frac{\partial \mathcal{O}}{\partial z_i} z_i + \frac{1}{2} \sum_{i,j} \frac{\partial^2 \mathcal{O}}{\partial z_i \partial z_j} z_i z_j$, where the derivatives are calculated using the error sets.

iii) repeat step i) and ii) many times, and interpret the many resulting values of \mathcal{O} as a statistical distribution of \mathcal{O} , with its one standard deviation representing the PDF-induced uncertainty of the observable \mathcal{O} .

Since the first- and second-order derivatives (*i.e.* $\frac{\partial \mathcal{O}}{\partial z_i}$ and $\frac{\partial^2 \mathcal{O}}{\partial z_i \partial z_j}$) can be readily calculated, the above bootstrap procedure can be quickly done.

The bootstrap procedure gives consistent uncertainty with Eq. (17). It is also convenient for calculating the correlation of the PDF-induced uncertainties between two physical observables \mathcal{O}_1 and \mathcal{O}_2 . One can calculate $(\delta\mathcal{O}_1)^2$, $(\delta\mathcal{O}_2)^2$ and $(\delta(\mathcal{O}_1 + \mathcal{O}_2))^2$ via either aforementioned method. The correlation is then easily acquired on the basis of its original definition of correlation:

$$\rho(\mathcal{O}_1, \mathcal{O}_2) = \frac{(\delta(\mathcal{O}_1 + \mathcal{O}_2))^2 - (\delta\mathcal{O}_1)^2 - (\delta\mathcal{O}_2)^2}{2\delta\mathcal{O}_1\delta\mathcal{O}_2} \quad (18)$$

Note that both the bootstrap method and Eq. (17) assume $\{z_i\}$ have independent gaussian distributions. As will be discussed in the next section, it is equivalent to the linear assumptions of Eq. (9), of which the uncertainty has been estimated as $\delta\mathcal{O}_E$. In conclusion, the total uncertainty on a physical observable \mathcal{O} is the quadratic combination of the original first-order uncertainties, the second-order uncertainties, and the non-linear uncertainty of $\delta\mathcal{O}_E$:

$$\begin{aligned} (\delta\mathcal{O}_{\text{total}})^2 &= \frac{1}{4} \sum_i [\mathcal{O}(S_{i+}) - \mathcal{O}(S_{i-})]^2 \\ &+ \frac{1}{32} \sum_i [\mathcal{O}(S_{i++}) + \mathcal{O}(S_{i--}) - 2\mathcal{O}(S_0)]^2 \\ &+ \frac{1}{32} \sum_{i \neq j} [\mathcal{O}(S_{j+}^{i+}) - \mathcal{O}(S_{j+}^{i-}) - \mathcal{O}(S_{j-}^{i+}) + \mathcal{O}(S_{j-}^{i-})]^2 \\ &+ \sum_r [\mathcal{O}(S_E(r)) - \mathcal{O}(S_0)]^2. \end{aligned} \quad (19)$$

The various contributions to the uncertainty can be numerically calculated with different settings. For example, in Eq. (14), we vary z_i and z_j from 0 to ± 1 . Actually the

variation can be any value as long as the denominator in Eq. (15) changes accordingly. Similarly, the calculations of second-order derivatives in Eq. (15) are not exclusive. Again, the non-linear uncertainty depends on the choice of ϵ_i and $\{a_i^r\}$. In a real global analysis, these settings should be determined with multiple factors taken into consideration, such as the particular data observables used in the global analysis, the experimental precision, the overall fitting quality, and the potential tensions between data. It also depends on the confidence level of a specific global analysis. For example, CTEQ-TEA gives its original uncertainty at 90% C.L. [2], while NNPDF directly estimates its uncertainty at 68.3% C.L. [10]. In this study we have focused on describing a general method instead of discussing the detailed choice of numerical settings, which should be decided in real global analysis on a case by case basis.

V. PSEUDO GLOBAL ANALYSIS

In this section, we introduce a pseudo global analysis to numerically test the improved Hessian method. We start with a set of parton densities taken from the CT18NNLO PDFs [2]. For valence u_V and d_V , the non-perturbative functions are:

$$\begin{aligned} f_q(x) &= a_0 x^{a_1-1} (1-x)^{a_2} P_a^V(y) \\ P_a^V(y) &= \sinh[a_3](1-y)^4 + \sinh[a_4]4y(1-y)^3 + \sinh[a_5]6y^2(1-y)^2 \\ &\quad + \left(1 + \frac{1}{2}a_1\right)4y^3(1-y) + y^4, \end{aligned} \quad (20)$$

where $y \equiv \sqrt{x}$. For both u_V and d_V , a_0 is fixed, following the flavor sum rules. We further require $a_1^{u_V} = a_1^{d_V}$ and $a_2^{u_V} = a_2^{d_V}$, as done in CT18 global analysis. For the sea quarks \bar{u} , \bar{d} , and $s = \bar{s}$, the non-perturbative functions are:

$$\begin{aligned} f_q(x) &= a_0 x^{a_1-1} (1-x)^{a_2} P_a^{\text{sea}}(y) \\ P_a^{\text{sea}}(y) &= (1-y)^5 + a_4 5y(1-y)^4 + a_5 10y^2(1-y)^3 \\ &\quad + a_6 10y^3(1-y)^2 + a_7 5y^4(1-y) + a_8 y^5, \end{aligned} \quad (21)$$

where $y \equiv 1 - (1 - \sqrt{x})^{a_3}$. We require $a_0^{\bar{u}} = a_0^{\bar{d}} = a_0^s = a_0^{\bar{s}}$, $a_1^{\bar{u}} = a_1^{\bar{d}} = a_1^s = a_1^{\bar{s}}$, $a_2^{\bar{u}} = a_2^{\bar{d}} = a_2^s = a_2^{\bar{s}}$, $a_3^{\bar{u}} = a_3^{\bar{d}} = a_3^s = a_3^{\bar{s}} = 4$, $a_4^{\bar{u}} = a_4^{\bar{d}} = a_4^s = a_4^{\bar{s}} = 1$, $a_5^{\bar{u}} = a_5^{\bar{d}} = a_5^s = a_5^{\bar{s}}$, and $a_6^{\bar{u}} = a_6^{\bar{d}} = a_6^s = a_6^{\bar{s}}$, following CT18. The distribution of the gluon is ignored in this test, since it would complicate the PDF analysis to add gluon contributions in the pseudo data. The charm quark is also ignored because it is highly correlated with the gluon. Therefore, we have 24 free parameters in total. Their central values are also set to the best fit of CT18NNLO at the initial energy scale $Q_0 = 1.3$ GeV [2], as listed in Tab. I. Figure 2 depicts $xf_q(x)$ for different quarks. We note that in this study, these pseudo PDFs will not be evolved to a high energy scale relevant to the pseudo data introduced below. These pseudo PDFs do not resemble any of the CT18 PDF sets. They are merely designed to simplify our discussions on

the effect of the second-order derivatives in Eq. (6) on the estimates of PDF-induced uncertainties.

	u_V	d_V	\bar{u}	\bar{d}	$s = \bar{s}$
a_0	3.385 (fixed)	0.490 (fixed)	0.414	0.414	0.288
a_1	0.763	0.763	-0.022	-0.022	-0.022
a_2	3.036	3.036	7.737	7.737	10.31
a_3	1.502	2.615	4 (fixed)	4 (fixed)	4(fixed)
a_4	-0.147	1.828	0.618	0.292	0.466
a_5	1.671	2.721	0.195	0.647	0.466
a_6	-	-	0.871	0.474	0.225
a_7	-	-	0.267	0.741	0.225
a_8	-	-	0.733	1 (fixed)	1 (fixed)

TABLE I. Values of parameters in the non-perturbative functions, taken from CT18NNLO.

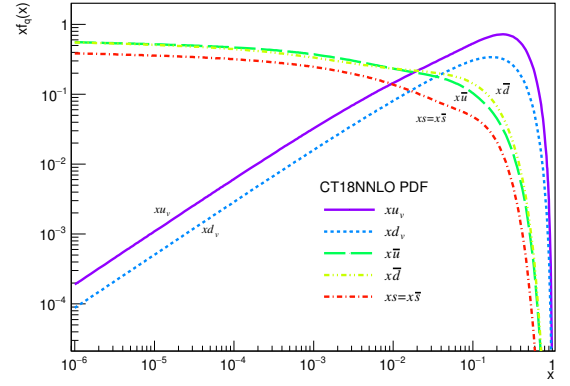


FIG. 2. $xf_q(x)$ for u_V , d_V , \bar{u} , \bar{d} and $s = \bar{s}$ in the pseudo global analysis.

A group of pseudo observables are also constructed according to the PDFs in Eq. (20) and Eq. (21). These observables, with uncertainties assigned, will be used as the data input in the pseudo global analysis. First, we introduce $\sigma_\gamma^{\text{DIS}}(x)$ and $\sigma_Z^{\text{DIS}}(x)$:

$$\begin{aligned} \sigma_\gamma^{\text{DIS}}(x) &= u_V(x) + 2\bar{u}(x) + 0.25 [d_V(x) + 2\bar{d}(x) + 2s(x)] \\ \sigma_Z^{\text{DIS}}(x) &= u_V(x) + 2\bar{u}(x) + 1.2 [d_V(x) + 2\bar{d}(x) + 2s(x)] \end{aligned} \quad (22)$$

as pseudo observables similar to the cross section measurements of the photon-exchange DIS process $\ell + p \rightarrow \gamma^* \rightarrow \ell + X$, and the Z -exchange DIS process $\ell + p \rightarrow Z/\gamma^* \rightarrow \ell + X$. The $q(x)$ functions are taken from Eq. (20) and Eq. (21), with $\{a_i\}$ values from Tab. I. The coefficient 0.25 (1.2) roughly reflects the strength difference between the down-type and up-type quarks coupling to γ (Z). Note that we take the definitions of $u \equiv u_V + \bar{u}$ and $d \equiv d_V + \bar{d}$, so that the \bar{u} and \bar{d} terms have a coefficient of 2. For simplicity, we ignore other contributions in a real calculation of the DIS process, such as the evolution of PDFs as a function of Q , the electroweak couplings and the higher order corrections. Although these

effects would significantly change the predictions on any physical observable, the main sensitivity to the particular parton information in those observables remains. For $\sigma_\gamma^{\text{DIS}}(x)$, 28 data points are calculated, with $x = 0.0001, 0.0002, 0.0003, 0.0004, 0.0005, 0.0006, 0.0007, 0.0008, 0.0009, 0.001, 0.002, 0.003, 0.004, 0.005, 0.006, 0.007, 0.008, 0.009, 0.01, 0.02, 0.03, 0.04, 0.05, 0.06, 0.07, 0.08, 0.09, 0.1$. For $\sigma_Z^{\text{DIS}}(x)$, 16 points are calculated, with $x = 0.01, 0.02, 0.03, 0.04, 0.05, 0.06, 0.07, 0.08, 0.09, 0.1, 0.15, 0.2, 0.25, 0.3, 0.35, 0.4$.

Similarly, we introduce the following cross section observables in proton-proton collisions: $\sigma_Z^{\text{pp}}(x_1, x_2)$, $\sigma_{W^+}^{\text{pp}}(x_1, x_2)$ and $\sigma_{W^-}^{\text{pp}}(x_1, x_2)$ as:

$$\begin{aligned}\sigma_Z^{\text{pp}}(x_1, x_2) &= [u_V(x_1) + \bar{u}(x_1)] \bar{u}(x_2) + [u_V(x_2) + \bar{u}(x_2)] \bar{u}(x_1) \\ &\quad + 1.2 [d_V(x_1) + \bar{d}(x_1)] \bar{d}(x_2) \\ &\quad + 1.2 [d_V(x_2) + \bar{d}(x_2)] \bar{d}(x_1) \\ &\quad + 1.2 \times 2 \times s(x_1) s(x_2) \\ \sigma_{W^+}^{\text{pp}}(x_1, x_2) &= 0.9 [(u_V(x_1) + \bar{u}(x_1)) \bar{d}(x_2)] \\ &\quad + 0.9 [(u_V(x_2) + \bar{u}(x_2)) \bar{d}(x_1)] \\ &\quad + 0.1 [(u_V(x_1) + \bar{u}(x_1)) s(x_2)] \\ &\quad + 0.1 [(u_V(x_2) + \bar{u}(x_2)) s(x_1)] \\ \sigma_{W^-}^{\text{pp}}(x_1, x_2) &= 0.9 [(d_V(x_1) + \bar{d}(x_1)) \bar{u}(x_2)] \\ &\quad + 0.9 [(d_V(x_2) + \bar{d}(x_2)) \bar{u}(x_1)] \\ &\quad + 0.1 \bar{u}(x_1) s(x_2) + 0.1 \bar{u}(x_2) s(x_1)\end{aligned}\quad (23)$$

They approximately represent the vector boson productions of $pp(q\bar{q}) \rightarrow Z/\gamma^* \rightarrow \ell^+ \ell^-$ and $pp(q_i \bar{q}_j) \rightarrow W^\pm \rightarrow \ell^\pm + \nu$. The momentum fractions x_1 and x_2 of the two initial quarks are connected by

$$x_{1,2} = \frac{\sqrt{M^2 + Q_T^2}}{\sqrt{s}} e^{\pm Y}$$

where M , Q_T and Y are the invariant mass, transverse momentum and rapidity of the bosons, respectively. In this work, M is set to 90 GeV, which is near the pole of the W and Z boson masses. Compared to M , the transverse momentum of the single vector boson production is usually small. Therefore Q_T is ignored in this work. \sqrt{s} is set to 13 TeV. To gain information for different x values, the cross section observables are calculated with different $|Y|$ values of 0.1, 0.3, 0.5, 0.7, 0.9, 1.1, 1.3, 1.5, 1.7, 1.9, 2.1, 2.4, 2.8, 3.2, 4.0. The corresponding x values range from 0.0001 to 0.38.

We also introduce a group of new experimental observables into the global fit, which are the proton structure parameters, P_u and P_d , factorized from the forward-backward asymmetry of the Drell-Yan process [11], and the boost asymmetry A_{boost} in the diboson process [12]. These asymmetry variables were recently proposed at hadron colliders which can provide unique information on the proton structure. The P_u and P_d parameters factorize the proton structure information in $pp(u\bar{u}) \rightarrow Z/\gamma^* \rightarrow \ell^+ \ell^-$ and $pp(d\bar{d}) \rightarrow Z/\gamma^* \rightarrow \ell^+ \ell^-$ events. The two light quark initial states can be decoupled because

the electroweak couplings of $u\bar{u}\text{-}Z$ and $d\bar{d}\text{-}Z$ are different. As a result, P_u and P_d separately provide the u and d quark information, which are mixed and indistinguishable in the measurement of the total cross section σ_Z^{pp} . A_{boost} is the asymmetry defined in the diboson production [12]. For example, in the $pp(u\bar{d}) \rightarrow W^+ \gamma \rightarrow \ell^+ \nu + \gamma$ process, the W^+ boson predominantly couples to the \bar{d} quark while the photon couples to the u quark. Consequently, the boost asymmetry $A_{\text{boost}}^{W^+ \gamma}$ has a positive large value, namely γ is more boosted than the W^+ boson, because the initial state parton luminosity $u(x_1) \bar{d}(x_2)$ is larger than $u(x_2) \bar{d}(x_1)$ for $x_1 > x_2$, etc. Therefore, the relative asymmetry between the initial-state parton luminosities $u(x_1) \bar{d}(x_2)$ and $u(x_2) \bar{d}(x_1)$ ($x_1 > x_2$) can be measured by comparing the energy or rapidity of the two bosons.

According to Ref. [11] and Ref. [12], the new pseudo observables can be constructed as:

$$\begin{aligned}P_u(x_1, x_2) &= [u_V(x_1) + \bar{u}(x_1)] \bar{u}(x_2) - [u_V(x_2) + \bar{u}(x_2)] \bar{u}(x_1), \\ P_d(x_1, x_2) &= [d_V(x_1) + \bar{d}(x_1)] \bar{d}(x_2) - [d_V(x_2) + \bar{d}(x_2)] \bar{d}(x_1), \\ A_{\text{boost}}^{W^+ \gamma}(x_1, x_2) &= [u_V(x_1) + \bar{u}(x_1)] \bar{d}(x_2) - [u_V(x_2) + \bar{u}(x_2)] \bar{d}(x_1), \\ A_{\text{boost}}^{W^- \gamma}(x_1, x_2) &= [d_V(x_1) + \bar{d}(x_1)] \bar{u}(x_2) - [d_V(x_2) + \bar{d}(x_2)] \bar{u}(x_1).\end{aligned}\quad (24)$$

In summary, 149 pseudo data points are introduced, corresponding to the DIS and Drell-Yan processes that are actually used in the PDF global analysis. For each data point, we assign a relative uncertainty of 3%. This precision is comparable to the HERA measurements and the LHC Drell-Yan measurements. For experimental results other than HERA and LHC, such as earlier DIS and semi-inclusive DIS measurements, their precisions are much lower. The experiments actually used in the PDF global analysis are summarized in Ref. [2]. Although these pseudo observables are only rough estimations rather than real calculations, they reflect the complexity of using multiple data inputs to determine the PDF shape parameters.

With the constructed PDFs, the pseudo observables and the assigned uncertainty, the Hessian matrix can be calculated accordingly. Since there are 24 free parameters in this test, the same number of eigenvectors and corresponding eigenvalues are acquired by diagonalizing the Hessian matrix. The eigenvalues in this test are shown in Fig. 3. As explained in Ref. [1], the eigenvalues in logarithmic scale rank as a line, reflecting the sensitivities of the input data. An eigenvector with large eigenvalue usually indicates that the information related to this eigenvector is well constrained by the input data. Otherwise, the input data has poor sensitivity to this eigenvector, leading to a small eigenvalue. Although data points in this analysis are much more than the free parameters being determined and the assigned uncertainty of 3% is quite small, there is still PDF information for certain x regions and parton flavors, for which no pseudo observable gives direct sensitivity. Therefore, some eigenvalues

are small compared to others. This also happens in a real PDF global analysis [2, 3, 9].

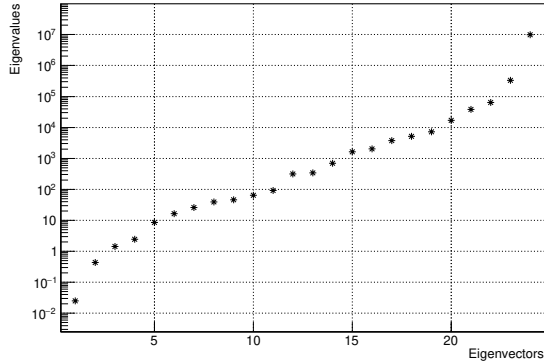


FIG. 3. 24 eigenvalues calculated from the Hessian matrix in the pseudo global analysis.

Once the Hessian matrix is diagonalized and the orthogonal displacements $\{z_i\}$ are acquired, one can look into the χ^2 - z_i relationship. It is a good numerical test of the linear assumptions in the global analysis. Usually, if the eigenvector represented by z_i is well constrained, χ^2 is expected to be an ideal quadratic function of z_i , giving $\chi^2(z_i = \pm n; z_j = 0 \text{ for } j \neq i) = n^2$. As discussed before, it also means the data inputs related to this eigenvector z_i are precise enough so that the corresponding T_α are approximately linear functions of the original parameters $\{a_i\}$ within small intervals. In Fig. 4, the χ^2 - z_i relationship for $i = 22$ and $i = 6$ are shown and compared, as an example. $i = 22$ is a typical eigenvector which has good linear approximation. Its eigenvalue is large at $\mathcal{O}(10^4)$. The χ^2 - z_i relationship follows a good quadratic approximation, so that $z_i = 1$ yields $\Delta\chi^2 = \chi^2 - \chi_{\min}^2 = 1$ corresponding to 1 standard deviation. For $i = 6$ however, it is an eigenvector which is not well constrained by data, resulting in a non-symmetric χ^2 - z_i relationship. In practice (also in this work), the 1 standard deviation in the uncertainty estimation is usually defined with the $\{z_i\}$ values which yields $\Delta\chi^2 = \chi^2 - \chi_{\min}^2 = 1$.

Following the method described in section IV, the uncertainty of any physical observable \mathcal{O} can be estimated according to Eq. (19). To numerically study the difference between the original Hessian method and the improved Hessian method, we compare the relative uncertainties of $xf_q(x)$ for u_V , d_V , \bar{u} , \bar{d} and s , which are shown in Fig. 5.

Fig. 5 shows that the non-linear uncertainty in this pseudo global analysis is much larger than the original uncertainty, especially in the large and small x region where no data can provide direct constraint. Even

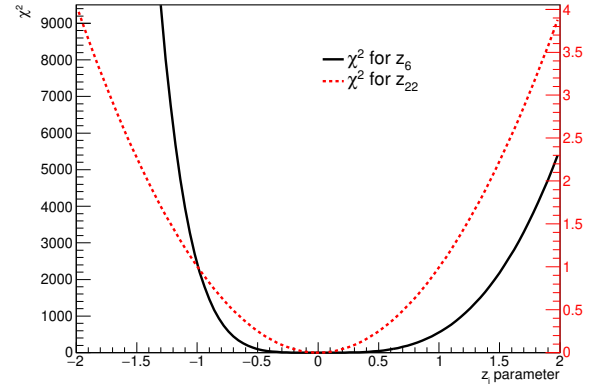


FIG. 4. χ^2 - z_i relationship for $i = 22$ (demonstrated in the right vertical axis) and $i = 6$ (demonstrated in the left vertical axis) eigenvectors.

though the pseudo data inputs in this work are generated using the non-perturbative functions exactly the same as that used in the pseudo theory calculations, the uncertainty of the choice of non-perturbative functions can still be reflected in the non-constrained area. The DIS-like observables are dominated by the valence quarks of u_V and d_V around the peak region of their distributions at $x \sim 0.1$, where the contributions of the sea quarks are relatively low. For the sea quarks however, there is no data predominated by them. Therefore, the valence pseudo quark PDFs are constrained more directly than the sea quark PDFs in this study. Consequently, the non-linear uncertainties for u_V and d_V are generally smaller than that for the sea quarks, as shown in Fig. 5. Moreover, the second-order uncertainty on the parton densities is not as significant as the non-linear uncertainty. If a physical observable contains information from multiple partons, the second-order uncertainties could be larger. In practice however, it could be fine not to compute the second-order uncertainty with thousands of second-order error sets for simplicity, especially when the non-linear uncertainty is already quoted.

In this work, the total uncertainties in the pseudo global analysis is several times larger than the original ones. According to the study from the CTEQ-TEA PDFs, the original uncertainties have to be enlarged corresponding to $\Delta\chi^2 = 37$, at the 68% confidence level, to cover the difference of using various non-perturbative functions, which also leads to a total uncertainty several times larger. The MSHT20 PDF gives a similar conclusion. In their studies, the PDF uncertainty is defined by a dynamic tolerance which effectively corresponds to $\Delta\chi^2 \sim 10$, giving the final uncertainty about 3 times larger than the original one. As a conclusion, the non-linear effect in the Hessian method is essential according to today's experimental precisions.

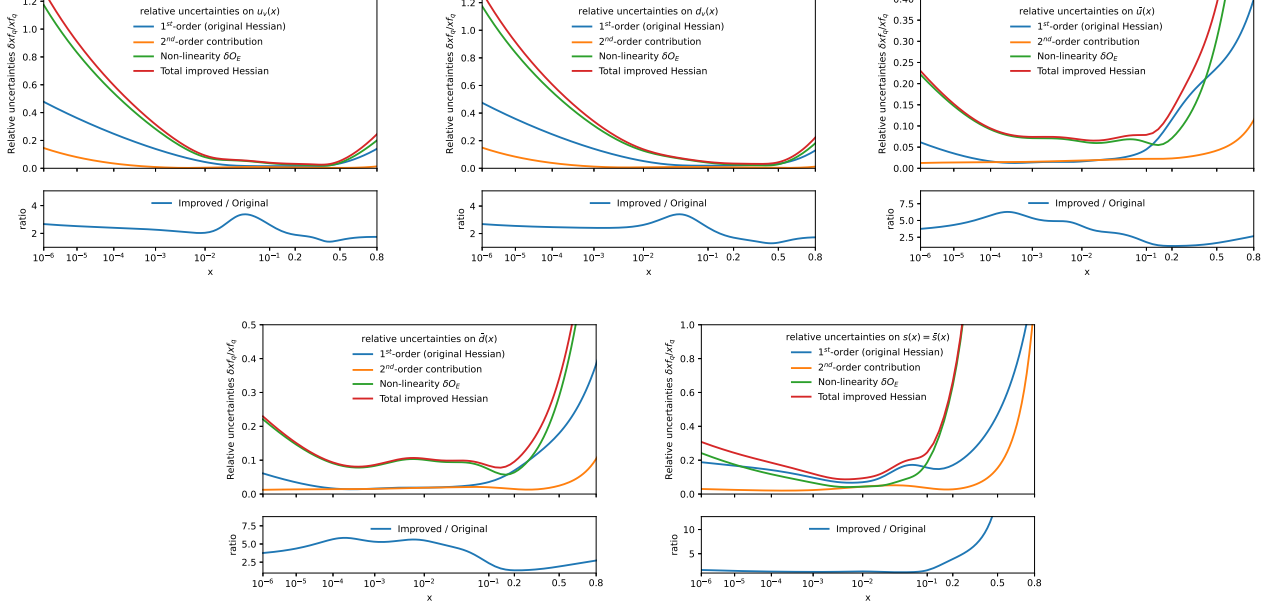


FIG. 5. Relative uncertainties on $xf_{u_V}(x)$, $xf_{d_V}(x)$, $xf_{\bar{u}}(x)$, $xf_{\bar{d}}(x)$ and $xf_s(x)$. Comparison includes the contribution of the first-order derivatives which is estimated from the original Hessian method (blue curves), the uncertainty of $\delta\mathcal{O}_E$ which estimates the non-linearity of $T_\alpha(a_i)$ (green curves), the uncertainty of the second-order derivatives additional to the first-order contributions (orange curves), and the total uncertainty from the improved Hessian method which is the quadratic sum of the previous three (red curves). The lower panel in each plot gives the ratio of the total uncertainty from the improved Hessian method to the original Hessian method.

ACKNOWLEDGEMENT

This work was supported by the National Natural Science Foundation of China under Grant No. 11721505, 11875245, 12061141005 and 12105275, and supported by the “USTC Research Funds of the Double First-Class Initiative”. This work was also supported by the U. S. National Science Foundation under Grant No. PHY-2310291.

Appendix: PDF-induced uncertainty on physical observables

In this section, we give the detailed calculation of Eq. (17). Rewrite Eq. (6) as:

$$\begin{aligned}\mathcal{O}(z_i) &= \mathcal{O}(z_i^0) + \sum_i A_i + \frac{1}{2} \sum_{i \neq j} B_{ij} \\ A_i &= \frac{\partial \mathcal{O}}{\partial z_i} z_i + \frac{1}{2} \frac{\partial^2 \mathcal{O}}{\partial z_i^2} z_i^2 \\ B_{ij} &= \frac{\partial^2 \mathcal{O}}{\partial z_i \partial z_j} z_i z_j\end{aligned}\quad (25)$$

The standard deviation of A_i can be calculated as:

$$\begin{aligned}V[A_i] &= E[A_i^2] - E[A_i]^2 \\ &= E\left[\left(\frac{\partial \mathcal{O}}{\partial z_i}\right)^2 z_i^2\right] + E\left[\frac{\partial \mathcal{O}}{\partial z_i} \frac{\partial^2 \mathcal{O}}{\partial z_i^2} z_i^3\right] \\ &\quad + E\left[\left(\frac{1}{2} \frac{\partial^2 \mathcal{O}}{\partial z_i^2}\right)^2 z_i^4\right] - E[A_i]^2\end{aligned}\quad (26)$$

where $V[X]$ and $E[X]$ corresponds to the standard deviation and mathematical expectation. Note that $E[z_i^2] = 1$, $E[z_i^3] = 0$ and $E[z_i^4] = 3$ for the gaussian distribution z_i . Therefore, we have

$$V[A_i] = \left(\frac{\partial \mathcal{O}}{\partial z_i}\right)^2 + \frac{1}{2} \left(\frac{\partial^2 \mathcal{O}}{\partial z_i^2}\right)^2. \quad (27)$$

Similarly, the standard deviation of B_{ij} is:

$$V[B_{ij}] = E[B_{ij}^2] - E[B_{ij}]^2 = \left(\frac{\partial^2 \mathcal{O}}{\partial z_i \partial z_j}\right)^2 \quad (28)$$

Given the fact that the A_i and B_{ij} terms are uncorrelated since they contain independent gaussian distributions, the standard deviation of \mathcal{O} is simply the sum of $V[A_i]$ and $V[B_{ij}]$, which are positive values. Consequently, the inclusion of second-order derivative terms always increases the size of the PDF-induced uncertainty in the physical observable. Furthermore, including only the second-order diagonal terms generally underestimates the uncertainty.

* yangsq@ustc.edu.cn

- [1] J. Pumplin, D. Stump, R. Brock, D. Casey, J. Huston, and J. Kalk, Phys. Rev. D **65**, 014013 (2001).
- [2] Tie-Jiun Hou, Jun Gao, T. J. Hobbs *et al.*, Phys. Rev. D **103**, 014013 (2021).
- [3] S. Bailey, T. Cridge, L. A. Harland-Lang, A. D. Martin, R. S. Thorne, Eur. Phys. J. C **81**, 341 (2021).
- [4] Carl Schmidt, Jon Pumplin, and C.-P. Yuan, Phys. Rev. D **98** 094005 (2018).
- [5] Sayipjamal Dulat, Tie-Jiun Hou, Jun Gao *et al.*, Phys. Rev. D **93**, 033006 (2016).
- [6] Kari J. Eskola, Petja Paakkinen, Hannu Paukkunen, Eur. Phys. J. C **79**, 511 (2019).
- [7] R. G. Roberts, The Structure of the proton: Deep inelastic scattering. Cambridge University Press, 1990.
- [8] R. Blankenbecler and S. J. Brodsky, Phys. Rev. D **10**, 2973 (1974).
- [9] H. Abramowicz *et al.* (H1 and ZEUS) Collaborations, Eur. Phys. J. C **75**, 580 (2015).
- [10] R. D. Ball *et al.* (NNPDF), Eur. Phys. J. C **82**, 428 (2022).
- [11] Siqu Yang, Yao Fu, Minghui Liu, Liang Han, Tie-Jiun Hou and C.-P. Yuan, Phys. Rev. D **106**, 033001 (2022).
- [12] Siqu Yang, Mingzhe Xie, Yao Fu, Zihan Zhao, Minghui Liu, Liang Han, Tie-Jiun Hou and C. P.-Yuan, Phys. Rev. D **106**, L051301 (2022).